TECHNICAL REPORT ARLCD-TR-82025

COMPARISON OF THE OPTICAL REFLECTIVITY OF A SHOCK FRONT IN LIQUID WATER AND IN LIQUID NITROMETHANE

PAUL HARRIS
ARRADCOM

HENRI-NÖEL PRESLES
UNIVERSITY DE POITIERS
FRANCE

NOVEMBER 1982

US ARMY ARMAMENT RESEARCH AND DEVELOPMENT COMMAND
LARGE CALIBER
WEAPON SYSTEMS LABORATORY
DOVER, NEW JERSEY

UNCLASSIFIED

SECURITY CLASSIFICATION OF THIS PAGE *(When Data Entered)*

REPORT DOCUMENTATION PAGE		READ INSTRUCTIONS BEFORE COMPLETING FORM
1. REPORT NUMBER Technical Report ARLCD-TR-82025	2. GOVT ACCESSION NO.	3. RECIPIENT'S CATALOG NUMBER
4. TITLE *(and Subtitle)* COMPARISON OF THE OPTICAL REFLECTIVITY OF A SHOCK FRONT IN LIQUID WATER AND IN LIQUID NITROMETHANE		5. TYPE OF REPORT & PERIOD COVERED FY82 6. PERFORMING ORG. REPORT NUMBER
7. AUTHOR(s) Paul Harris, ARRADCOM Henri-Nöel Presles, University de Poitiers, France		8. CONTRACT OR GRANT NUMBER(s) Project 1L161101A91A
9. PERFORMING ORGANIZATION NAME AND ADDRESS ARRADCOM, LCL Nuclear and Fuze Div (DRDAR-LCN Dover, NJ 07801		10. PROGRAM ELEMENT, PROJECT, TASK AREA & WORK UNIT NUMBERS
11. CONTROLLING OFFICE NAME AND ADDRESS ARRADCOM, TSD STINFO Div (DRDAR-TSS) Dover, NJ 07801		12. REPORT DATE November 1982 13. NUMBER OF PAGES 26
14. MONITORING AGENCY NAME & ADDRESS*(if different from Controlling Office)*		15. SECURITY CLASS. *(of this report)* Unclassified 15a. DECLASSIFICATION/DOWNGRADING SCHEDULE

16. DISTRIBUTION STATEMENT *(of this Report)*

Approved for public release; distribution unlimited.

17. DISTRIBUTION STATEMENT *(of the abstract entered in Block 20, if different from Report)*

18. SUPPLEMENTARY NOTES

19. KEY WORDS *(Continue on reverse side if necessary and identify by block number)*

Shock waves
Shock front
Shock structure
Explosives

20. ABSTRACT *(Continue on reverse side if necessary and identify by block number)*

Shock front optical reflectivity data for liquid water at 5.8 kbar and for liquid nitromethane at 6.0 kbar are analyzed with a reflectivity theory containing rereflection within the shock front. Comparison of the analyses for water and for nitromethane leads to the conclusion that additional physics is necessary to explain the nitromethane data. It is suggested that the experimental-theoretical discrepancy for nitromethane is optical-path-length dependent, and that discrepancy is possibly due to thermal fluctuations related to explosive chemistry.

DD FORM 1 JAN 73 1473 EDITION OF 1 NOV 65 IS OBSOLETE

UNCLASSIFIED

SECURITY CLASSIFICATION OF THIS PAGE *(When Data Entered)*

ACKNOWLEDGMENTS

The authors thank H. Simonnet and Y. Sarazin (both of the University de Poitiers) for experimental assistance. They are also indebted to F. H. Stillinger (Bell Telephone Laboratories) and A. Karo (Lawrence Livermore National Laboratories) for helpful discussions.

CONTENTS

FIGURES

INTRODUCTION

For the past two years the collaborative effort between the University of Poitiers and ARRADCOM has been concentrating on the physics of the shock front rise time (structure) in liquids. Liquid water has been the primary vehicle for that study.

Recent success in obtaining optical reflectivity data for liquid nitromethane and in writing a more complete reflectivity theory (rereflection has now been included) have shifted the program's emphasis from the shock front rise time to the systematic differences observed in the shock front reflectivity of water and nitromethane (for assumed comparable rise times). This is the first report of the more complete theory and those systematic differences.

Any systematic difference between the shock front reflectivities of water and nitromethane could be very important from both fundamental and applied viewpoints. The results presented in this report suggest the possibility that explosive-related chemistry is already occurring within the shock front thickness of liquid nitromethane, and that the effects of that chemistry can be observed in the optical reflectivity results. Were such a possibility to become fact, one would have a new tool for observing and controlling detailed explosive properties in terms of molecular structure and composition. From a fundamental point of view, the role of liquid structure and composition on shock front structure is fascinating in its own right.

MULTIPLE REFLECTION THEORY

In our previous work (ref 1) the effect of multiple reflections was neglected. For large reflectivities (e.g., 20% at an 82° optical angle of incidence in water) such a neglect can lead to difficulties. Multiple reflections are considered here by means of a perturbative approach.

Consider a differential region of varying indexes of refraction as shown in figure 1.

In the absence of multiple reflections, the differential reflected amplitude is given by

$$dE_r = \frac{E}{2}\left(\frac{dn}{n}\right)(1 \pm \tan^2\theta) \qquad (1)$$

where θ is the angle of incidence (measured with respect to the normal to the surface of dn), and the +, - signs refer to perpendicular, or parallel (to the plane of incidence) optical polarizations, respectively.

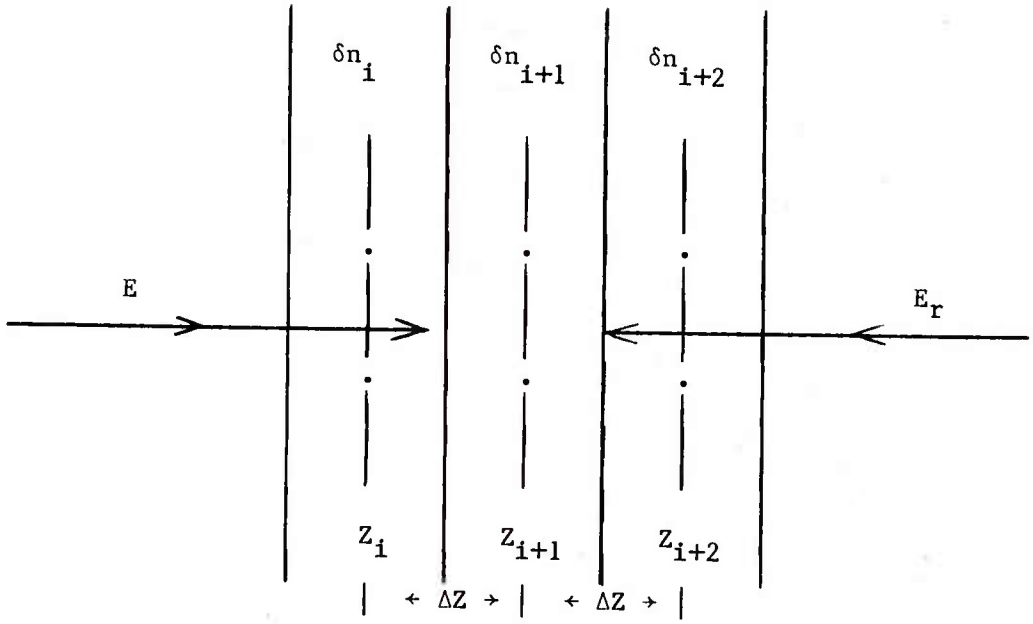

Figure 1. Incoming and reflected fields, E and E_r, respectively, impinging on a slab of differential index of refraction δn_{i+1}, centered at Z_{i+1}, and of width ΔZ

Applying equation 1 to both E and E_r in figure 1 gives

$$dE_r(Z_{i+1}) = \frac{1}{2}\left[\frac{\delta n_{i+1}}{n(Z_{i+1})}\right]\left[1 \pm \tan^2\theta(Z_i + \frac{\Delta Z}{2})\right]E(Z_i + \frac{\Delta Z}{2}) + \\ - \frac{1}{2}\left[\frac{\delta n_{i+1}}{n(Z_{i+1})}\right]\left[1 \pm \tan^2\theta(Z_{i+1} + \frac{\Delta Z}{2})\right]E_r(Z_{i+1} + \frac{\Delta Z}{2}) \quad (2)$$

Upon expanding terms such as $E_r(Z_{i+1} + \frac{\Delta Z}{2})$ in equation 2,

$$E_r(Z_{i+1} + \frac{\Delta Z}{2}) = E_r(Z_{i+1}) + \frac{dE_r}{dZ}\Big|_{i+1}(\frac{\Delta Z}{2}) + \frac{1}{2}\frac{d^2E_r}{dZ^2}\Big|_{i+1}(\frac{\Delta Z}{2})^2 + \cdots, \quad (3)$$

gives to lowest order

$$\frac{dE_r}{dZ} = \frac{(E - E_r)}{2n}(\frac{dn}{dZ})(1 \pm \tan^2\theta) \quad (4)$$

Equation 4 simply says that, to lowest order, $(E - E_r)$ replaces E in equation 1 when rereflection is taken into account. This result could, of course, have been guessed.

Rewrite equation 4 as

$$\left[\frac{d}{dZ} + \left(\frac{1}{2n}\frac{dn}{dZ}\right)(1 \pm \tan^2\theta)\right]E_r = \frac{E}{2n}\frac{dn}{dZ}(1 \pm \tan^2\theta) \tag{5}$$

and make the transformations

$$E_r \equiv F(Z)e^{f(Z)}, \quad E \equiv G(Z)e^{f(Z)} \tag{6}$$

Substituting equation 6 into equation 5 gives

$$\frac{dF}{dZ} = \frac{G}{2n}\frac{dn}{dZ}(1 \pm \tan^2\theta) \tag{7}$$

if f(Z) is taken to satisfy the differential equation

$$\frac{df}{dZ} = -\frac{1}{2n}\frac{dn}{dZ}(1 \pm \tan^2\theta) \tag{8}$$

Thus, when (-f) is taken to be the reflected amplitude associated with unit amplitude input electric field, F may be viewed as the reflected amplitude associated with field strength G <u>in a space where rereflection of F does not occur</u>. That is the beauty of the transformation given by equation 6; one can solve for F exactly as in the simple case (ref 1) where multiple reflections are not important.

For a shock front beginning at Z = 0, the reflectivity, R, is given by

$$R = \left|\frac{E_r(0)}{E(0)}\right|^2 = \left|\frac{F(0)}{G(0)}\right|^2 \tag{9}$$

Thus F(0) and G(0) determine the reflectivity.

Poynting's theorem for the reflection problem being considered here can be written as

$$C_o(|E(0)|^2 - |E_r(0)|^2)\sin\theta_o = \tag{10}$$

$$= C(|E|^2 - |E_r|^2)\sin\theta$$

where C_o is the velocity of light in the preshocked medium. For

$$v(Z) \equiv C(Z)e^{2f(Z)} \tag{11}$$

Equation 10 becomes

$$v_o(|G(0)|^2 - |F(0)|^2)\sin\theta_o = \tag{12}$$

$$= v(|G|^2 - |F|^2)\sin\theta$$

Applying Snell's law, $n\sin\theta = n_o\sin\theta_o$, to equation 12 gives

$$\left|\frac{G(Z)}{G(0)}\right|^2 = \left\{\frac{ne^{f(0)}}{n_o e^{f(Z)}}\right\}^2 \left\{1 - \left|\frac{F(0)}{G(0)}\right|^2\right\} + \left|\frac{F(Z)}{G(0)}\right|^2 \tag{13}$$

One now proceeds as in reference 1, where multiple reflections were neglected, by defining fractional optical phase angles, γ_A and γ_B, by

$$\frac{G(Z)}{G(0)} \equiv \left|\frac{G(Z)}{G(0)}\right| e^{2\pi i\gamma_A} \tag{14}$$

$$\frac{dF}{G(0)} \equiv \left(d\left|\frac{F}{G(0)}\right|\right)e^{2\pi i\gamma_B} + 2\pi i\left|\frac{F}{G(0)}\right| e^{2\pi i\gamma_B} d\gamma_B \tag{15}$$

Upon rewriting equation 13 to lowest order in $\left|\frac{F}{G(0)}\right|$,

$$\left|\frac{G}{G(0)}\right| = \left\{\frac{ne^{f(0)}}{n_o e^{f(Z)}}\right\}\left\{1 - \left|\frac{F(0)}{G(0)}\right|^2\right\}^{1/2}\left\{1 + \left|\frac{F}{G(0)}\right|^2\right\}^{1/2} \tag{16}$$

and substituting that along with equations 14 and 15 into equation 7 gives

$$\frac{d\left|\frac{F}{G(0)}\right|}{\sqrt{1 + \left|\frac{F}{G(0)}\right|^2}} = \left(\frac{dn}{2n}\right)\left\{1 - \left|\frac{F(0)}{G(0)}\right|^2\right\}^{1/2}(1 \pm \tan^2\theta)\cos\{2\pi(\gamma_A - \gamma_B)\} \tag{17}$$

The solution proceeds by solving equations 8 and 17 along with an equation for $(\gamma_A - \gamma_B)$.

Because F and G in equation 7 appear with the absence rereflection, writing down equations for their fractional phase angles γ_A and γ_B is relatively simple.*

$$d\gamma_B = -\frac{\cos\theta}{\lambda}\, dZ \tag{18a}$$

$$d\gamma_A = \frac{\cos\theta}{\lambda}\, dZ \tag{18b}$$

Integrating equations 18 while using Snell's law and $\lambda = \lambda_{oo} n^{-1}$ (with λ_{oo} being the optical wavelength in vacuum) gives

$$(\gamma_A - \gamma_B) = \frac{2}{\lambda_{oo}} \int_0^Z \left\{n^2(Z') - n_o^2 \sin^2\theta_o\right\}^{1/2} dZ' \tag{19}$$

Again, the foot of the shock front is assumed to begin at Z = 0, and again our problem is solved to first order in rereflection by simultaneously solving equations 8, 17, and 19.

SOLUTIONS WITH REREFLECTION

It is simple to show that

$$(1 \pm \tan^2\theta) = \left\{ \begin{array}{ll} +, & \dfrac{n^2}{n^2 - n_o^2 \sin^2\theta_o} \\ -, & \dfrac{n^2 - 2n_o^2 \sin^2\theta_o}{n^2 - n_o^2 \sin^2\theta_o} \end{array} \right\} \tag{20}$$

so that integrating equation 8 from n_o to n gives

$$f_+(Z) = -\frac{1}{4} \ell n \left\{\frac{n^2 - n_o^2 \sin^2\theta_o}{n_o^2 - n_o^2 \sin^2\theta_o}\right\} \tag{21}$$

---

* A rereflection contribution to G(Z) would, in principle, complicate the phase γ_A (Z).

$$f_-(Z) = - f_+(Z) + \ell n\left(\frac{n_o}{n}\right) \tag{22}$$

Equation 19 has previously (ref 2) been evaluated for the special case of a constant gradient in the index of refraction,

$$n = n_o + (\Delta n)_f \frac{Z}{L} \tag{23}$$

where L is the shock front thickness and $(\Delta n)_f$ is the total change in index of refraction across the shock front. That equation 19 result for the special case of equation 23 is

$$(\gamma_A - \gamma_B) = \frac{n_o^2 L}{\gamma_{oo}(\Delta n)_f}\left\{(m+1)^2\sqrt{1 - \left(\frac{\sin\theta_o}{m+1}\right)^2} - \cos\theta_o + \right.$$
$$\left. - \sin^2\theta_o \ell n\left[\frac{(m+1)\left\{1 + \sqrt{1 - \left(\frac{\sin\theta_o}{m+1}\right)^2}\right\}}{1 + \cos\theta_o}\right]\right\} \tag{24}$$

where

$$m \equiv \frac{n}{n_o} - 1 \tag{25}$$

has been used. m is the most convenient parameter to use for the numerical integration of the right hand side of equation 17.

As Z goes from Z = 0 to the top of the shock, $\left|\frac{F}{G(0)}\right|$ goes from $R^{1/2}$ to 0 (reflection ceases at the top of the shock). Thus

$$\int_{\left|\frac{F(0)}{G(0)}\right|}^{0} \frac{d\left|\frac{F}{G(0)}\right|}{\sqrt{1 + \left|\frac{F}{G(0)}\right|^2}} = \ell n\left\{R^{1/2} + \sqrt{1 + R}\right\} \tag{26}$$

where equation 9 has been used, and equation 17 becomes

$$\frac{\ell n\left\{R^{1/2} + \sqrt{1 + R}\right\}}{\sqrt{1 - R}} = - \frac{1}{2n_o} \int_{n_o}^{n_f} dn \left\{\frac{e^{f(0)}}{e^{f(Z)}}\right\}(1 \pm \tan^2\theta)\cos\{2\pi(\gamma_A - \gamma_B)\} \tag{27}$$

Equation 27 should be compared with the previous (ref 1, 2) result where rereflection and F(Z) on the right hand side of equation 12 are neglected. That previous result is

$$R = \sin\left[\frac{1}{2n_o} \int_{n_o}^{n_f} dn\ (1 \pm \tan^2\theta)\cos\{2\pi(\gamma_A - \gamma_B)\}\right] \tag{28}$$

In the limit of $n \to n_o$ and $R \to 0$ equations 27 and 28 give indentical results.

Let $I_\pm$ denote the right hand side of equation 27. To order $R^{3/2}$, equation 27 may then be written as

$$R^{1/2}\ (1 + \frac{R}{3}) = -\ I_\pm \tag{29}$$

which becomes (to order R^2)

$$R^2 + \frac{3}{2}R - \frac{3}{2}\ I_\pm^{\ 2} = 0 \tag{30}$$

Solving equation 30 for R to order $I_\pm^{\ 4}$ then gives

$$R = I_\pm^2 - \frac{2}{3}\ I_\pm^4 \tag{31}$$

Equation 31, along with equations 21, 22, and 24, represents the final result of this section. To the algebraic order considered, the result is consistent with a first order correction for multiple reflections (i.e., for the presence of rereflection) and finite reflectivity (e.g., F(Z) in the right hand side of equation 12 taken to be non-zero). The algebraic accuracy of equation 31 is such that inclusion of the next higher order term for R in equation 29 is equivalent to a 1% reflectivity calculational error when R = 0.2 (i.e., 20% reflection).

It is a fairly simple task to evaluate $I_\pm$ numerically by means of partitions and a cyclic computer program. Indeed, a 19-partition integration program was run on a TRS-80 handheld computer with each calculation point taking approximately 5 minutes. The results of those calculations are shown and discussed in the next section. The calculational error associated with 19 as compared 39 program steps throughout the entire range of experimental interest is less than 1%.

EXPERIMENTAL AND THEORETICAL RESULTS

The experimental data points shown in figures 2, 3, and 4 are the results of an experimental program at the Laboratory for Energetics and Detonation (C.N.R.S. Lab 193) of the University of Poitiers. That experimental program is supported by the Centre National de la Recherche Scientifique (C.N.R.S.) of France. The theory presented in the previous section is supported by the U.S. Army through the In-House Laboratory Independent Research (ILIR) Program within the Large Caliber Weapons Systems Laboratory (LCL) of ARRADCOM.

The experimental data points were obtained with the small light-gas canon facility at the University of Poitiers. A stabilized argon laser operating at 4145Å was used to illuminate the shock front, and an 8-mm diameter, 10-namosecond rise time, silicon photodiode was used to measure the calibrated reflectivity. The pressure determination (5.8 kbar in water and 6.0 kbar in nitromethane) was measured to within 5%, while the reflectivity record was read to within 10%.

The authors have previously compared (ref 1) experiment with theory (without multiple reflections) for water. With multiple reflections (fig. 2), $\beta_{\perp} \leq 0.1$ fits the data fairly well, while a somewhat larger value of $\beta_{\parallel}$ appears to be necessary for the parallel to the plane-of-incidence optical polarization. In the absence of multiple reflections, the theory fits both optical polarizations equally well ($\beta \leq 0.1$). While it cannot be said at this time whether the difference in agreement between theory and experiment for the two optical polarizations in water has a real physical basis, in principle, the two optical polarizations should not quite "see" the same thing.

Rahman and Stillinger (ref 3) have demonstrated (by computer molecular dynamics) a finite lifetime for shear waves in liquid water (e.g., $\sim 0.4 \times 10^{-12}$ sec for a shear wavelength of ~13Å). The implication of that finite lifetime is the initial one-dimensional strain's becoming hydrostatic only after the shock front (i.e., after the shock plateau) has been reached. The 0.4×10^{-12} sec lifetime is consistent with a shock front rise time in water of $\sim 10^{-12}$ sec as has independently been determined (ref 4) from shock polarization theory and experiment. Thus, the perpendicular optical polarization case (with $\underline{E}$ perpendicular to the direction of shock propagation), and the parallel polarization case (where $E\sin\theta$ is the component of $\underline{E}$ parallel to the direction of shock propagation) would not "see" identical physical phenomena.

The data and theory (with rereflection included) for liquid nitromethane are shown in figure 3. The systematic loss of agreement between theory and experiment, for both polarizations, with increasing angle of incidence (decreasing grazing angle) is clear and graphic. The approximately 50% difference between theory and experiment at 8 degrees grazing angle is well beyond theoretical and experimental uncertainty and error.

The optical path length through the shock front is given by $(2L/\cos\theta)$ where L is the shock front thickness. The systematic worsening of agreement between theory and experiment suggests the possible existence of an optical path length effect in the reflectivity measurements. In turn, an optical path length effect

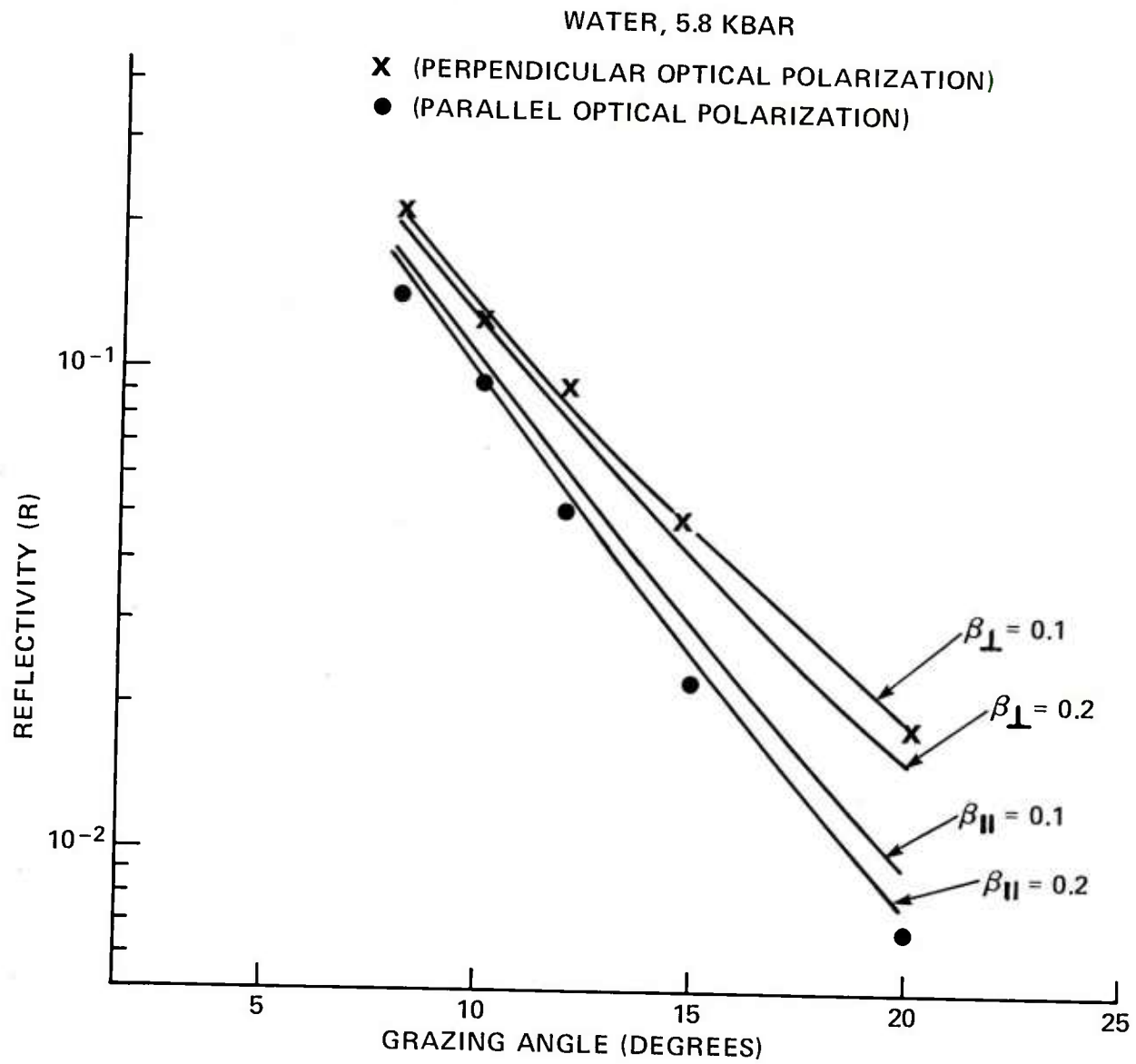

Figure 2. Experimental and theoretical (from equation 31) reflectivities for m_f = 0.0394. $\beta = n_o L/\lambda_{oo}$. Solid lines are theory, and X and • are experimental data points. The subscripts on β inidcate the optical polarization. For liquid water. Grazing angle is $(\theta_o - 90°)$

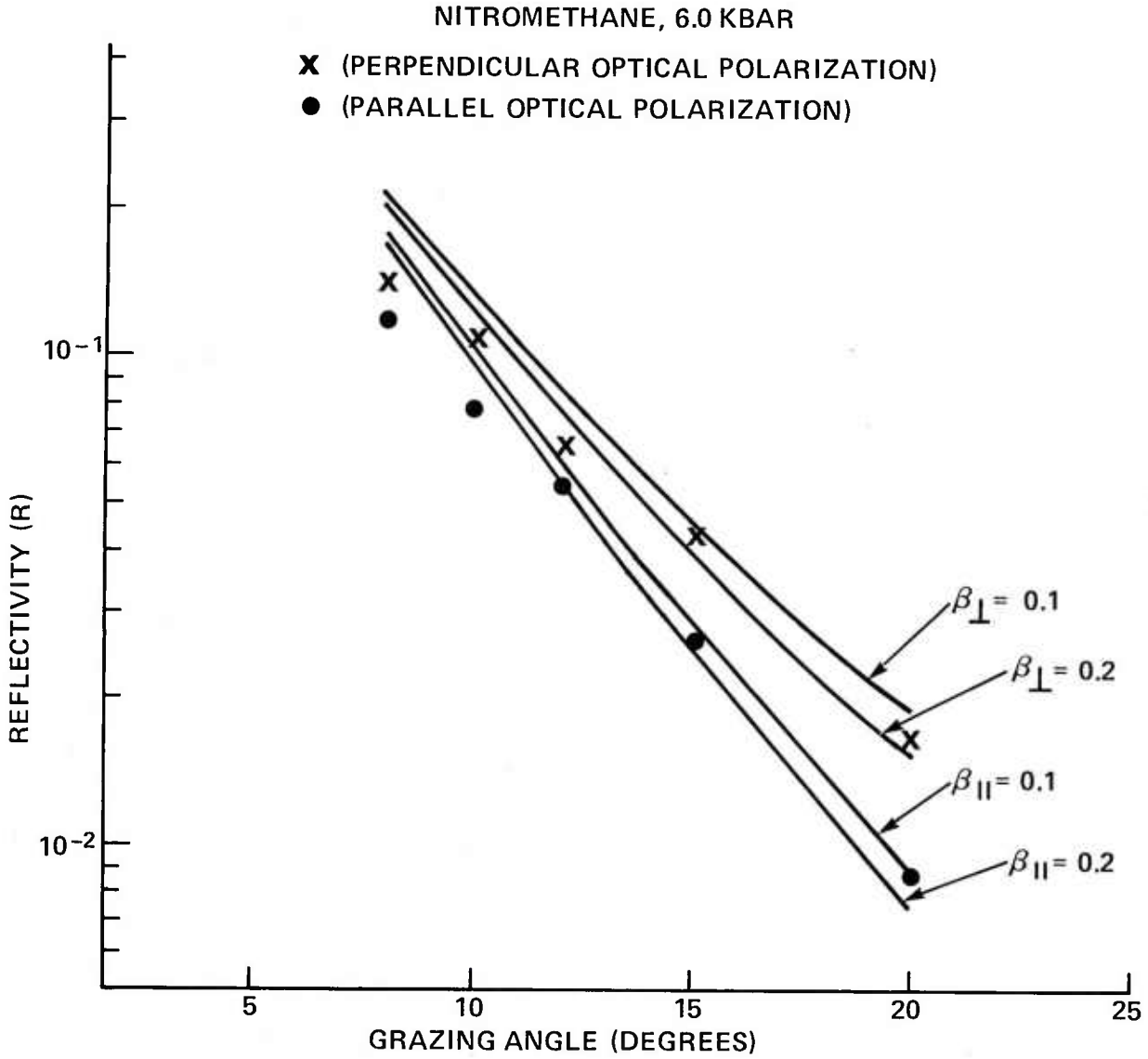

Figure 3. Experimental and theoretical (from equation 31) reflectivities for m_f = 0.0394. $\beta = n_o L/\lambda_{oo}$. Solid lines are theory, and X and ● are experimental data points. The subscripts on β indicate the optical polarization. For liquid nitromethane. Grazing angle is $(\theta_o - 90°)$

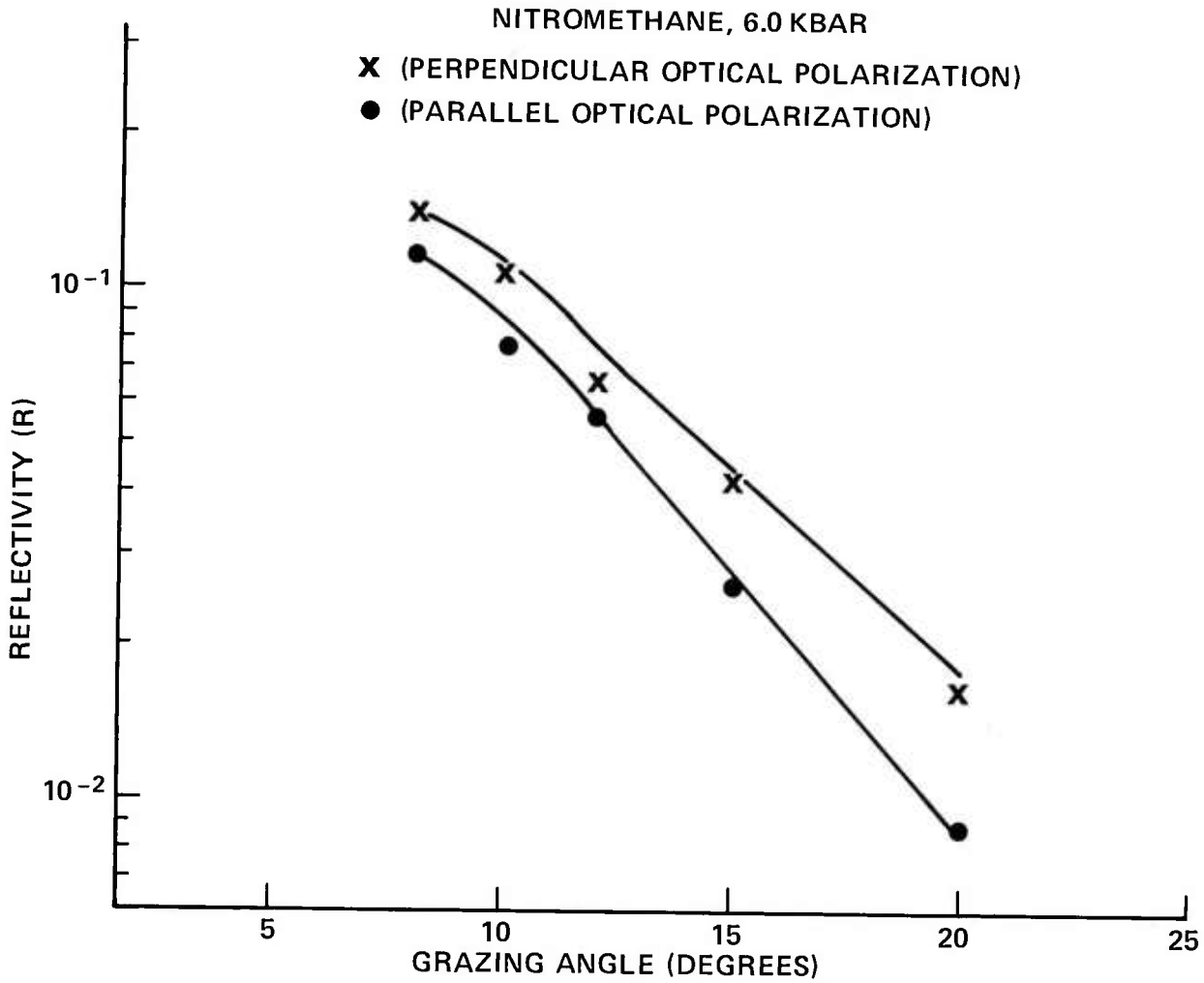

Figure 4. X and ● are experimental data points. Solid curves are the effect of "Thermal Fluctuations" added to the $\beta = 0.1$ curves of figure 3. For liquid nitromethane. Grazing angle is $(\theta_o - 90°)$

suggests the possible existence of an optical-scattering-related fluctuation phenomenon.

Since nitromethane is an explosive, it is conceivable that the reflectivity data are demonstrating the existence of chemically related thermal fluctuations within the shock front. Toops has reported (ref 5) on the temperature dependence of the index of refraction for liquid nitromethane. His observations give

$$\frac{dn}{dT} = -4.5 \times 10^{-4}\ {}^{0}C^{-1} \tag{32}$$

so that a $(\Delta T) > 0$ fluctuation will decrease the measured index of refraction contribution at the fluctuation site.

Consider a reflectivity, R, approximately given by

$$R^{1/2} = \frac{(\Delta n)_f}{2n_o}\,(1 \pm \tan^2\theta) \tag{33}$$

and a fluctuation effect on $(\Delta n)_f$ given by

$$(\Delta n)_f = (\Delta n)_f^{(o)}\,(1 + \alpha(T)h) \tag{34}$$

where $h = 2L\cos^{-1}\theta$ is the optical path length. If $(\Delta R)_\theta$ is taken as the change in reflectivity caused by the thermal fluctuations characterized by α, and if $(\alpha h) < 1$, then

$$(\Delta R)_{\theta_1} \approx (\Delta R)_{\theta_2}\left(\frac{1 + \tan^2\theta_1}{1 + \tan^2\theta_2}\right)\frac{\cos\theta_2}{\cos\theta_1} \tag{35}$$

If $(\Delta R)_\theta$ is taken as the difference between experimental and theoretical values for $\beta_{\perp,11} = 0.1$ at $\theta = 82°$, then

$$\perp(\Delta R)_{82^0} = -5.5 \times 10^{-2} \tag{36a}$$

$$11(\Delta R)_{82^0} = -4.4 \times 10^{-2} \tag{36b}$$

Substituting equations 36a and 36b into equation 35 yields the solid curves shown in figure 4. Clearly a path length dependent subtractive contribution to Δn by means of equations 33 through 35 serves to facilitate the agreement between theory and experiment.

DISCUSSION AND CONCLUSIONS

The most striking aspect of the theoretical and experimental results presented in this report is the distinct difference between theoretical and experimental agreement for liquid water and liquid nitromethane. While the agreement for water is not perfect, the agreement for nitromethane is clearly lacking in the absence of some angle of incidence dependent effect such as that proposed by equations 33 and 34. Liquid nitromethane is an explosive and it seems reasonable to postulate explosive-related chemistry (although 6 kbar is approximately an order of magnitude less than room-temperature shock initiation pressure) as the mechanism for the $\alpha(T)h$ term of equation 34.

If the experimental-theoretical discrepancy shown in figure 3 can be attributed to explosive-related chemical effects, as seems very possible, the authors believe that the attribution would be a first for the physics of explosive (energetic) media. If explosive-related chemistry is the mechanism for proposed thermal fluctuations, then the experimental-theoretical discrepancy should increase with increasing shock pressure. Time and further experiments will tell.

$m_f = 0.0394$ was used for both water at 5.8 kbar, and nitromethane at 6.0 kbar. For liquid nitromethane at 20°C, from Toops (ref 5) and Hardesty (ref 6),

$$\Delta n = 0.338 \, (\rho - \rho_o) \tag{37}$$

where ρ is mass density. From Enig and Petrone (ref 7) ρ (6 kbar) = 1.304 g cm^{-3} so that $(\Delta n)_f = 0.0544$. The preshock value of $n_o = 1.385$ then gives $m_f = 0.0393$.

For water, from Zeldovich, et al (ref 8),

$$\Delta n = 0.334 \, (\rho - 1)$$

From $\Delta\rho = 0.1575$ g cm^{-3} (an extrapolation of the Rice and Walsh (ref 9) data) and $n_o = 1.334$ one finds $m_f = 0.0394$. As a 0.3% change in m_f can barely be seen on a plot of theoretical results, the same m_f value was used in characterizing the index of refraction change in both liquids. Similarly a 10°C shock-induced temperature change has a negligible effect on the theoretical predictions of equation 32.

REFERENCES

1. P. Harris and H.-N. Presles, J. Chem. Phys., vol 74, 1981, p 6864.

2. P. Harris and H.-N. Presles, "The Optical Reflectivity of a Shock Front," Technical Report of the Laboratoire d'Energetique et de Detonique, Universite de Poitiers, January 1981.

3. A. Rahman and F. H. Stillinger, Phys. Rev. A, vol 10, 1974, p 368.

4. P. Harris and H.-N. Presles, J. Chem. Phys., November 1982.

5. E. E. Toops, Jr., J. Phys. Chem., vol 60, 1956, p 304.

6. D. R. Hardesty, J. Appl. Phys., vol 47, 1976, p 1994.

7. J. W. Enig and F. J. Petrone, Phys. Fluids, vol 9, 1966, p 398.

8. Ya. B. Zel'dovich, S. B. Kormer, M. V. Sinitsyn, and K. B. Yushko, Sov. Phys. Dokl., vol 6, 1961, p 494.

9. M. H. Rice and J. M. Walsh, J. Chem. Phys., vol 26, 1957, p 824.

DISTRIBUTION LIST

Commander
U.S. Army Armament Research
and Development Command
ATTN: DRDAR-TD, D. Gyorog
DRDAR-TSS (5)
DRDAR-LC, J. Frasier
DRDAR-LCN, H. Grundler
P. Harris (50)
Harry Fair
T. Gora
W. Doremus
G. Vezzolli
DRDAR-LCE, R. Walker
Louis Avrami
F. Owens
C. Capellos
DRDAR-GCL
Dover, NJ 07801

Director
Lawrence National Laboratory
ATTN: Frank E. Walker
A. M. Karo
Livermore, CA 94550

Stanford Research Institute
Poulter Laboratories
ATTN: William J. Murri
D. R. Curran
R. K. Linde
Menlo Park, CA 94025

Sandia National Laboratory
ATTN: Walter Hermann
Robert Graham
D. B. Hayes
J. Gover
William Benedick
R. E. Hollenbach
L. D. Bertholf
P.O. Box 5800
Albuquerque, NM 87116

Washington State University
ATTN: George Duvall
G. R. Fowles
George Swan
Pullman, WA 99163

Commander
U.S. Naval Surface Weapons Center
Explosion Dynamics Division
ATTN: D. John Pastine
S. J. Jacobs
J. Forbes
James Goff
White Oak, MD 20910

Commander
U.S. Army Research Office
ATTN: J. Chandra
C. Boghosian
I. Lefkowitz
P.O. Box 12211
Research Triangle Park, NC 27709

Commander
U.S. Army Research and Standardization
Group (Europe)
P.O. Box 65
FPO 09510

National Bureau of Standards
ATTN: Donald Tsai
Henry Prask
Gaithersburg, MD 20760

California Institute of Technology
ATTN: Thomas J. Ahrens
Lien G. Yang
Pasadena, CA 91109

Department of Chemistry and
Chemical Engineering
ATTN: H. G. Drickamer
Urbana, IL 60436

Commander
U.S. Army Armament Research
and Development Command
DRDAR-BLT, Philip Howe
Y. K. Huang
George E. Hauver
DRDAR-BLB, Donald Eccleshall
D. F. Strenzwilk
DRDAR-BLI, George Adams
I. May
DRDAR-BL, Robert F. Eichelberger
DRDAR-TSB-S (Tech Library)
Aberdeen Proving Ground, MD 21005

Commander
Benet Weapons Laboratory, LCL
ATTN: T. E. Davidson
DRDAR-LCB-TL (Tech Library)
Watervliet, NY 21289

University of Delaware
Department of Physics
ATTN: Ferd E. Williams
W. B. Daniels
Newark, DE 19711

Director
Defense Technical Information Center
ATTN: Accessions Division (12)
Cameron Station
Alexandria, VA 22314

Union Carbide Corporation
Tarrytown Technical Center
ATTN: Jaak Van Den Sype
Tarrytown, NY 10591

McDonnel Douglas Astronautics
ATTN: John Watcher
Harvey Berkowitz
5301 Bolsa Avenue
Huntington Beach, CA 92647

Systems, Science, and Software
ATTN: H. E. Read
P.O. Box 1620
La Jolla, CA 92037

U.S. Army Materials & Mechanics
Research Center
ATTN: John F. Dignam
John Mescall
D. P. Dandekar
Building 131
Arsenal Street
Watertown, MA 02172

Lockheed Palo Alto Research Labs
ATTN: J. F. Riley
3251 Hanover Street
Palo Alto, CA 94304

Bell Telephone Labortories
ATTN: F. H. Stillinger
Murray Hill, NJ 07974

Director
Los Alamos Scientific Laboratory
ATTN: J. M. Walsh
Los Alamos, NM 87544

Commander
U.S. Army Missile Command
ATTN: Charles M. Bowden
Redstone Arsenal, AL 35809

University of Tennessee
ATTN: M. A. Breazeale
Dept of Physics and Astronomy
Knoxville, TN 37916

Princeton University
ATTN: A. C. Eringen
Princeton, NJ 08540

Carnegie Mellon Institute
of Technology
ATTN: Morton E. Gurtin
Bernard D. Coleman
Department of Mathematics
Pittsburgh, PA 15213

Brown University
ATTN: Robert T. Beyer
Department of Physics
Providence, RI 02912

Courant Institute of
Mathematical Sciences
ATTN: Library
New York University
New York, NY 10453

City College of the
City University of New York
ATTN: Harry Soodak
Department of Physics
139th Street & Convent Ave
New York, NY 10031

Queens College of the City
University of New York
ATTN: Arthur Paskin
Department of Physics
Flushing, NY 11300

SPIRE Corp
ATTN: Roger Little
Patriots Park
Redford, MA 01730

Director
U.S. Army Materiel Systems
Analysis Activity
ATTN: DRXSY-MP
Aberdeen Proving Ground, MD 21005

Commander/Director
Chemical Systems Laboratory
U.S. Army Armament Research
and Development Command
ATTN: DRDAR-CLJ-L
DRDAR-CLB-PA
APG, Edgewood Area, MD 21010

Commander
U.S. Army Armament Materiel
Readiness Command
ATTN: DRSAR-LEP-L
Rock Island, IL 61299

Director
U.S. Army TRADOC Systems
Analysis Activity
ATTN: ATAA-SL
White Sands Missile Range, NM 88002